

## SPECIAL FEATURES OF THE NOTHING ON INSULATOR TRANSISTOR SIMULATED WITH DIAMOND LATERAL ISLANDS

C. RAVARIU

Politehnica University of Bucharest, Faculty of Electronics, Department of Electronic Devices  
Circuits and Architectures, Splaiul Independentei 313, sect. 6, Bucharest, RO-060042, Romania,  
E-mail: *cristian.ravariu@upb.ro*

*Received March 16, 2018*

*Abstract.* A diamond on insulator structure based on the tunneling conduction thru a vacuum gap between source and drain is proposed as a continuity of previous studies. The Nothing On Insulator (NOI) cavity represents the main device body of this kind of transistors. The simulations reveal the diamond device work principle and extract the static characteristics accompanied by specific parameters accordingly to the diamond properties. The simulations establish a gate leakage current of 8 nA for the diamond NOI device *versus* 10  $\mu$ A in the silicon case, at the same biases. Non-uniform diamond surfaces with nano-grains or pipes are considered as some real technological aspects.

*Key words:* device physics, diamond nanostructure, tunneling.

### 1. INTRODUCTION

Besides to the silicon compounds, the C-related materials offer enhanced performances for multiple applications: CNTFETs, graphene devices, carbon nanotubes field emitters [1-4]. The miniaturization goal of the vacuum tubes recently reached to the vacuum nanotransistors in Si [5] or diamond transistor with field emission in vacuum, [6]. Additionally, SiC and Diamond are predicted to be the next materials for electronic devices able to minimize the leakage currents. Several green electronics scenario are envisaged, mainly as "end use efficiency" based on power saving, leakage current minimization that will save till 39% of the worldwide emission reduction by 2030, [7].

In a previous work, we presented a Diamond On Insulator transistor with a minor gap above a thin film that connect the source and drain islands, [8]. Subsequently, the thin film was thinned down up to few atomic layers [8] and then completely removed. At this stage a new device architecture was proposed in 2005 in Si [9] and timely optimized [10, 11]. Due to the Nothing cavity placed On Insulator support (NOI) as the main device body, this device was accepted to be called NOI transistor [12, 13]. Its conduction is solely based on the vacuum cavity tunneling. The device technology is difficult to be implemented in Si, as depicted

in a patent 2013, [14]. The NOI transistor implementation in diamond belongs to the future facilities, but its simulations are useful to reveal its special feature.

An international interest for this kind of transistors with vacuum nano-cavity starts in 2012, when a NASA research group, first time fabricated a vacuum nano-transistor in Si and demonstrated the Fowler-Nordheim tunneling conduction through a gap of 10 nm [15]. The experimental characteristics,  $SS = 1.4V/dec$ ,  $V_{DS} = 20V$ , [15] fit to the simulated NOI characteristics,  $SS = 650 mV/dec$ ,  $V_{DS} = 10V$ , [16]. An enthusiastic period follows, announcing in 2015 ultimate vacuum tubes [17], introducing the vacuum transistor as a device made of Nothing [18], transistorizing the Vacuum Tube, promising transistors with vacuum able to fill the terahertz gap, [18]. Obviously, the NOI transistor belongs to this vacuum nanotransistors class of international interest [5, 6, 13–18]. In this paper, the diamond-NOI device consists in two lateral diamond islands, separated by a “Nothing” region, onto an oxide support, Fig. 1.

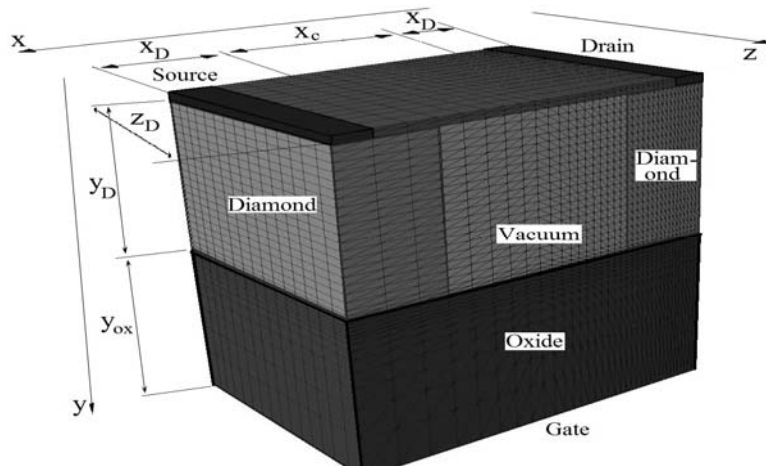


Fig. 1 – The diamond-NOI nano-device and notations.

In this paper the notations are:  $x_D$ ,  $y_D$ ,  $z_D$  – the diamond sizes on  $Ox$ ,  $Oy$  and respectively  $Oz$  directions,  $x_c$  – the cavity length on  $Ox$  axis,  $y_{ox}$  – the oxide thickness,  $N_{A,D}$  – the doping concentration in the p-type and respectively n-type diamond,  $Q_{ss}$  – the interface charge between oxide and diamond.

## 2. THE DIAMOND-NOI-SET-1 DEVICE SIMULATION

The target of this paper is to demonstrate by simulations the diamond-NOI work principle and to extract its parameters. The material property, interfacial and

bulk diamond parameters are adopted from Atlas/Silvaco library, [19]. In the first set of simulations, the diamond-NOI-Set-1 device has: a n-type diamond doping concentration of  $N_D = 7 \times 10^{20} \text{ cm}^{-3}$  for ohmic contacts with metals, oxide/diamond interface charge of  $10^{12} \text{ e/cm}^2$  and sizes  $x_D = 4 \text{ nm}$ ,  $y_D = 40 \text{ nm}$ ,  $y_{ox} = 20 \text{ nm}$ ,  $x_c = 2 \text{ nm}$  (Fig. 2). In next simulations results, Atlas expresses the currents in Amperes per  $1 \mu\text{m}$ .

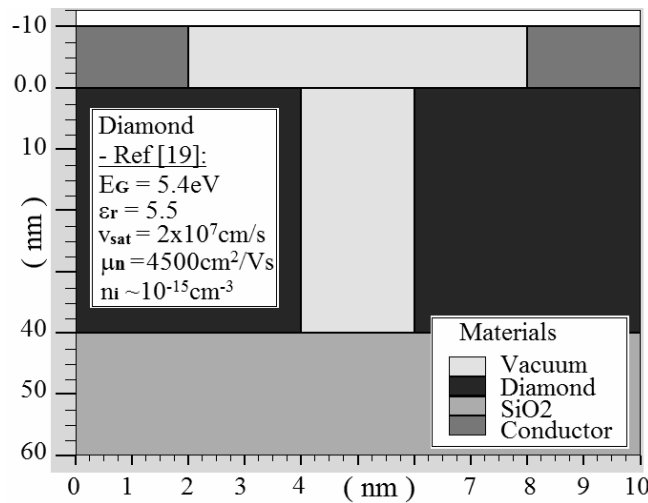


Fig. 2 – The diamond-NOI-Set-1 device with default material parameters for diamond from Atlas library.

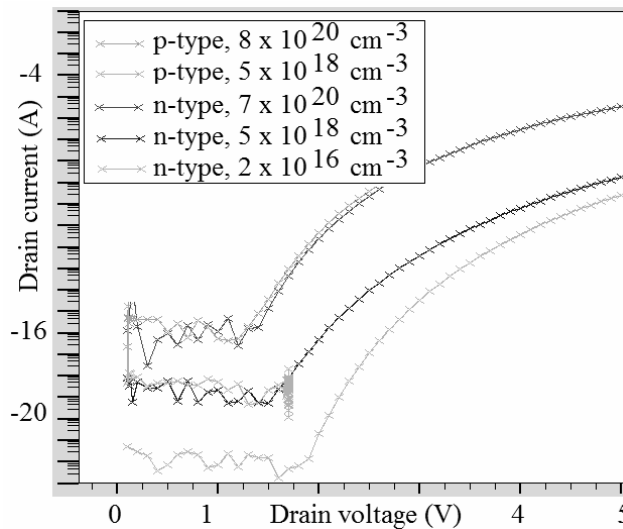


Fig. 3 – The  $I_D-V_D$  simulated curves for different doping types.

Accordingly with the previous study about the suitable model for a NOI device simulation [16], in this analysis the following models are applied: FNORD model for tunneling, CVT-Lombardi mobility model for non-planar devices, Fermi carrier distributions, Band Gap Narrowing for heavily doped diamond islands and Selberherr's ionization model for general purposes.

Over time, the diamond have an entire history in the impurification technology [20, 21]. To check the functionality of the diamond-NOI device for different doping types and levels of the lateral diamond islands, a short study is presented. The *Set-1* structure is biased at  $V_G = +8$  V,  $V_S = 0$  V, while the drain voltage is ramped from 0 V to 5 V, monitoring the drain current (Fig. 3).

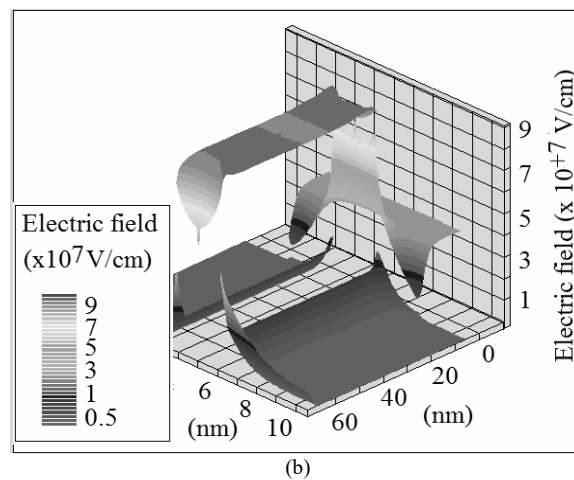
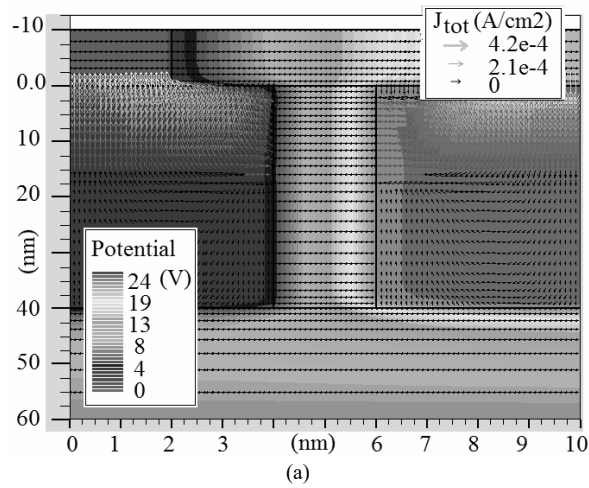


Fig. 4 – a) The electric field and current vectors; b) The electric field distribution, at  $V_S = 0$  V,  $V_G = 8$  V,  $V_D = 20$  V.

When p-type  $5 \times 10^{18} \text{ cm}^{-3}$  or below doping is used in simulation, the current tends to a noisy limit level. Higher currents are offered by the n-type diamond highly doped around  $N_D = 5 \times 10^{18} \text{ cm}^{-3}$ . If the real technology requires a decreased n-doping, the current also decreases, but keeps the same  $I_D$ - $V_{DS}$  characteristic shape, indicating two firm ON, OFF states (Fig. 3). The ON current decreases from 8000 nA at  $N_D = 7 \times 10^{20} \text{ cm}^{-3}$ , to 2 nA at  $N_D = 5 \times 10^{18} \text{ cm}^{-3}$ , to 0.4 nA at  $N_D = 2 \times 10^{16} \text{ cm}^{-3}$ .

Some validations of the current transport through the Diamond-NOI-Set-1 variant, are available in Fig. 4a. The total current density shows maximum vectors near the metallic source/drain contacts when n-type doping is used. The current lines go through the vacuum cavity, which possesses high electric field, able to trigger the tunneling for the useful drain current (Fig. 4b).

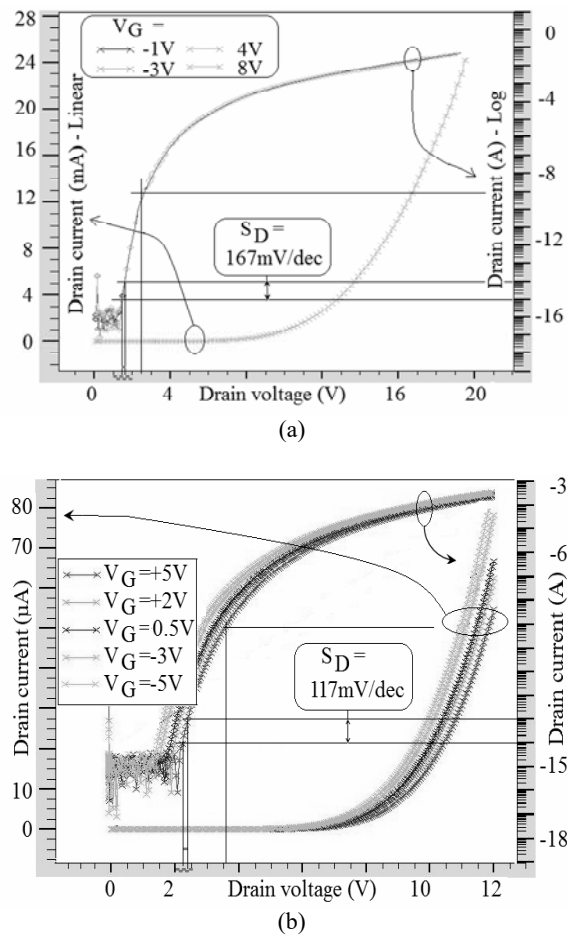


Fig. 5 – The simulated output characteristics of Set-1 with: a)  $y_{\text{ox}} = 20 \text{ nm}$ ; b)  $y_{\text{ox}} = 15 \text{ nm}$ .

A maximum field of  $7 \times 10^7$  V/cm occurs at  $V_S = 0$  V,  $V_G = 8$  V,  $V_D = 20$  V in the upper vacuum cavity, near the diamond corners. This allows the electrons discharge in vacuum, attesting the useful tunneling. The island corners with more than  $1.7 \times 10^7$  V/cm – the critical electric field in diamond, enters in breakdown regime, providing further electrons releasing.

Figure 5a presents the simulated characteristics of the best diamond-NOI-Set1 variant with n-type doping of  $N_D = 7 \times 10^{20}$  cm<sup>-3</sup> and  $y_{ox} = 20$  nm, biased at  $V_S = 0$  V,  $V_G = 8$  V,  $V_D = 0 \div 20$  V.

The main target of this analysis is fulfilled: the Fowler-Nordheim exponential emission  $I_D - V_{DS}$  characteristics for the Diamond-NOI device occurs (Fig. 5). Obviously, pushing the drain voltage to +20 V, the drain current increases to 24 mA for  $N_D = 7 \times 10^{20}$  cm<sup>-3</sup> (Fig. 5a).

Admitting similar definitions of the drain threshold voltage in Diamond as in Si [12],  $V_{DST}$  as the drain voltage that raises the current to 1 nA and the drain sub-threshold slope as drain drop voltage per 1 decade of current increasing in sub-threshold conditions, result:  $V_{DST} = 2.5$  V and  $S_D = 167$  mV/dec, Fig. 5a for diamond-NOI device. The gate bias doesn't modulate the drain current. The method to increase the gate action was elsewhere depicted [13]. If a thinner oxide is used,  $y_{ox} = 15$  nm, the drain current starts to be modulated by the gate bias (Fig. 5b). All parameters prosper at negative gate voltages:  $V_{DST} = 3.2$  V and  $S_D = 117$  mV/dec at  $V_G = +5$  V and  $V_{DST} = 2.2$  V and  $S_D = 100$  mV/dec at  $V_G = -5$  V, besides to  $I_D = 20$   $\mu$ A at  $V_{DS} = 10$  V (Fig. 5b). These simulations emphasize moderate optimizations *versus* the Si-NOI-15nm case with:  $V_{DST} = 2.3$  V and  $S_D = 170$  mV/dec, [12], but promising performances *versus* the vacuum diamond nano-transistor with  $V_{ON} = 40$  V and  $I_D = 0.3$   $\mu$ A at  $V_{DS} = 460$  V [6] or vacuum Si transistor with swing of  $S = 4$  V/dec [15].

### 3. THE DIAMOND-NOI-SET-2 STRUCTURE WITH ROUGH WALLS

In the second set of simulations, the Diamond-NOI-Set2 device has sizes, charges and dopings as Set1, but considers some nano-grains on the diamond walls, as roughnesses real effect. In Fig. 6, the un-regular diamond surface gets three nano-grains of 1 nm. The presence of these nano-grains is expected to maintain the Fowler-Nordheim tunneling. The nano-grains presence means much more corners; hence, the useful tunneling is rapidly initiated. The electric field exhibits three peaks of  $6 \times 10^7$  V/cm in the "Nothing" region and values less than  $6 \times 10^6$  V/cm in diamond, at  $V_S = 0$  V,  $V_G = -5$  V,  $V_D = 7$  V, as is identified in the color legend from Fig. 7. The current density vectors show that the main carriers flow is confined through the source-drain nano-grains.

The simulations from Fig. 8 reveal an interesting behavior: the nano-grains presence doesn't affect the drain current of the Si-NOI or similar diamond-NOI

device. But the NOI structure with diamond islands benefits on a gate current decreasing from  $40 \mu\text{A}$  in Si-NOI-Set2 to  $10^{-9} \div 10^{-8} \text{A}$  in diamond-NOI-Set2, for  $10 \text{ V} < V_D < 12 \text{ V}$  (Fig. 8).

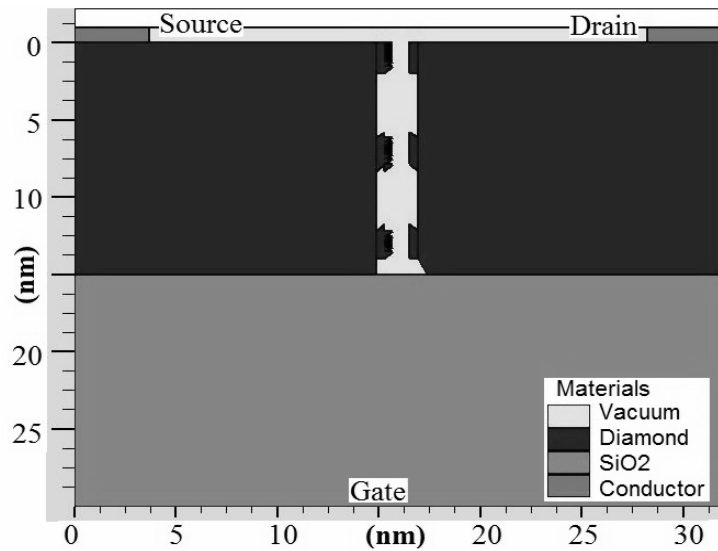


Fig. 6 – The Diamond-NOI-Set2 device with 3 nano-grains.

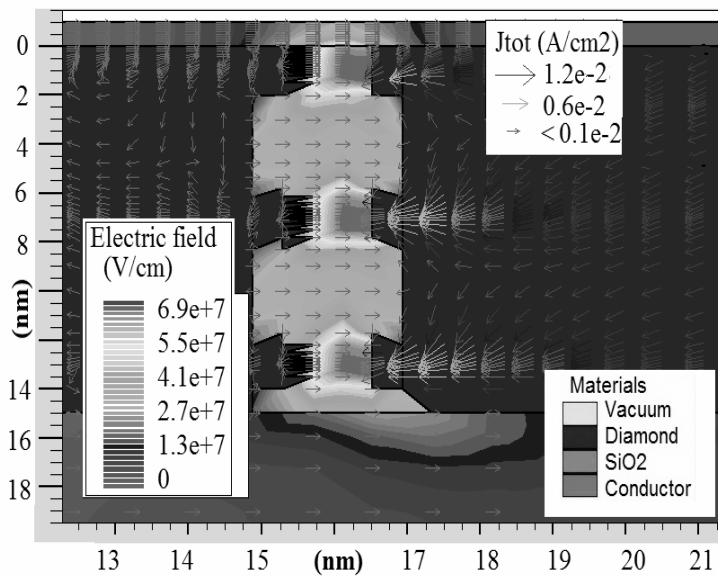


Fig. 7 – The total electric field at  $V_G = -5 \text{ V}$ ,  $V_D = 7 \text{ V}$  – detail inside Diamond-NOI-Set2.

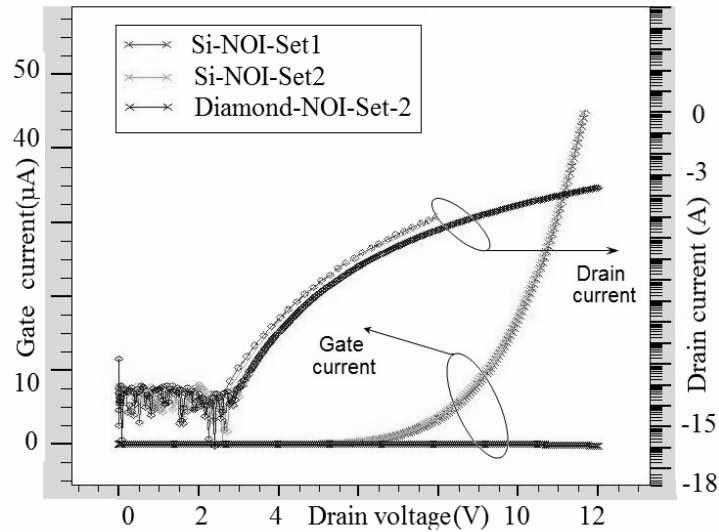


Fig. 8 – The drain and gate characteristics, comparatively presented, at  $V_G = -3$  V.

#### 4. DISCUSSIONS AND POSSIBLE ACCIDENTS

The diamond-NOI-Set-2 device offers the minimum gate leakage current and maximum drain current capability, *versus* any silicon case.

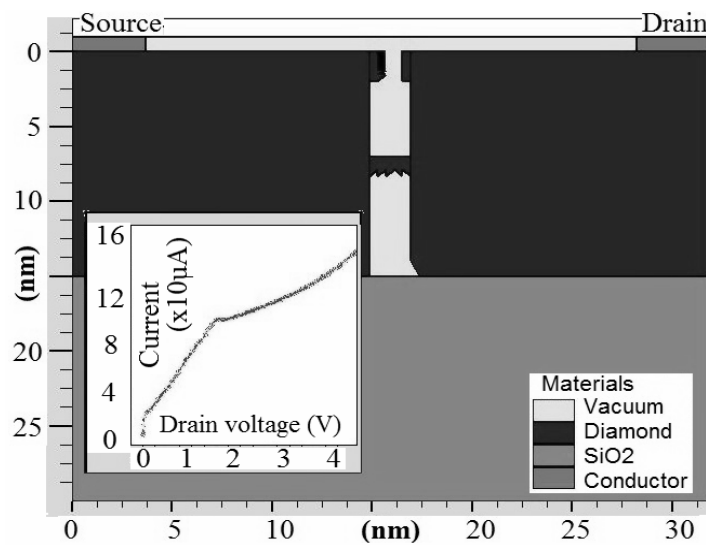


Fig. 9 – The NOI structure with two touched nano-grains as a pipe; inset – the  $I_D-V_{DS}$  simulated characteristics.

The experimental measurements found roughness of such nano-layers is typically 2–5 nm [22] – so that the 2-nm gap could be easily closed. This situation is simulated if two nano-grains accidentally touch during the technological processing (Fig. 9). Unfortunately, this pipe act as a drain-source shortcut, accompanied by a current confinement thru the pipe. The characteristics shape is changing, indicating immediately after 0 V a drain current increasing (Fig. 9 – inset). It is expected the characteristics evolve toward a  $I_D$ – $V_{DS}$  characteristic with saturation of current if the pipe thickness exceeds 5 nm, in agreement with other studies [23].

## 5. CONCLUSIONS

The paper presented a nano-device composed by two diamond islands separated by 2 nm gap. The studied configurations of the Diamond-NOI device started by *Set-1*, with flat diamond walls on 20 nm oxide and continued by *Set-2* with rough walls with nano-grains on 15 nm oxide.

The main advantage of the diamond-NOI device instead the Silicon-NOI variant consists in lower gate leakage currents. In the same bias conditions, the low intrinsic carrier concentration in diamond allows  $I_G = 8$  nA for diamond-NOI case and  $I_G = 12$   $\mu$ A for Si-NOI case, at  $V_{DS} = 10$  V. This feature is important, because if the oxide can be thinned down without the gate leakage danger, the transistor effect can be enhanced to increase the gate voltage action on the drain currents. The maximum drive currents of 70  $\mu$ A were simulated at  $V_{DS} = 11.5$  V and  $V_G = -5$  V if the diamond islands get n-type doping concentration around  $10^{20}$  cm<sup>-3</sup>. If a pipe arises between source/drain nano-islands, immediately the current is confined thru this pipe: the drain current stronger increases with the drain voltage, deviates from the Fowler-Nordheim law and evolve toward a characteristic with saturation when the pipes are thicker.

**Acknowledgements.** This work is developed by grants of the Romanian National Authority for Scientific Research and Innovation, CNCS/CCCDI UEFISCDI: PN-III-P4-ID-PCE-2016-0480, project number 4/2017-TFTNANOEL and PN-III-P2-2.1-PED-2016-0427 project number 205PED/2017-DEMOTUN.

## REFERENCES

1. M.E. Barbinta-Patrascu, N. Badea, C. Ungureanu, C. Pirvu, V. Ifimie, and S. Antohe, *Photophysical studies on biocomposites based on carbon nanotubes and chlorophyll-loaded biomimetic membranes*, Rom. Rep. Phys. **69**, 604 (2017).
2. T. Iwasaki, H. Kato, T. Makino, M. Ogura, D. Takeuchi, S. Yamasaki, and M. Hatano, *High-Temperature Bipolar-Mode Operation of Normally-Off Diamond JFET*, IEEE Journal of the Electron Devices Soc. **5**(1), 95–99 (2017).

3. I. Calina, M. Demeter, E. Badita, E. Stancu, A. Scarisoreanu, and C. Vancea, *Reduction of freestanding graphene oxide films using continuous wave laser*, Rom. Rep. Phys. **69**, 504 (2017).
4. R. Majidi, M. Saadat, and S. Davoudi, *Electronic properties of doped porous graphene and biphenylene carbon: A density functional theory study*, Rom. Rep. Phys. **69**, 509 (2017).
5. J.W. Han, J.S. Oh, and M. Meyyappan, *Cofabrication of Vacuum Field Emission Transistor (VFET) and MOSFET*, IEEE Transactions on Nanotechnology **13**(3), 464–468 (2014).
6. K. Subramanian, W.P. Kang, and J.L. Davidson, *A Monolithic Nanodiamond Lateral Field Emission Vacuum Transistor*, IEEE Electron Device Lett. **29**(11), 1259–1261 (2008).
7. S. Shikata, *Single crystal diamond wafers for high power electronics*, Diamond and Related Materials **65**(3), 168–175 (2016).
8. C. Ravariu, A. Rusu, F. Udrea, and F. Ravariu, *Simulation results of some Diamond on Insulator nano-MISFETs*, Diamond and Related Materials **15**(4–8), 777–782 (2006).
9. C. Ravariu, *A NOI – nanotransistor*, Proc. IEEE Int. Conf. of Semiconductors, Sinaia, Romania, 2005, pp. 65–68.
10. C. Ravariu, *The implementation methodology of the real effects in a NOI nanostructure aided by simulation and modelling*, Simulation Modeling Practice and Theory **18**(9), 1274–1285 (2010).
11. C. Ravariu, *Semiconductor Materials Optimization for A TFET Device with Nothing Region on Insulator*, IEEE Trans. on Semiconductor Manufacturing **26**(3), 406–413 (2013).
12. C. Ravariu, *Compact NOI Nano-Device Simulation*, IEEE Transactions on VLSI Systems **22**(8), 1841–1844 (2014).
13. C. Ravariu, *Gate Swing Improving for the Nothing on Insulator Transistor in Weak Tunneling*, IEEE Transactions on Nanotechnology **16**(6), 1115–1121 (2017).
14. C. Ravariu, *Field effect transistors with a cavity on insulator NOI and its technology*, Patent Number: RO126811-A0, OSIM (2013).
15. J. Han, J. Oh, and M. Meyyappan, *Vacuum nanoelectronics: Back to the future?-Gate insulated nanoscale vacuum channel transistor*, Appl. Physics Lett. **100**, 213505 (2012).
16. C. Ravariu, *Deeper Insights of the Conduction Mechanisms in a Vacuum SOI Nanotransistor*, IEEE Trans. on Electron Devices **63**(8), 3278–3283 (2016).
17. M. Armstrong, *The quest for the ultimate vacuum tube*, IEEE Spectrum **25**, 29–35 (2015).
18. J. Han and M. Meyyappan, *Introducing the vacuum transistor: a device made of Nothing*, IEEE Spectrum, NASA Researcher group **24**, 25–29 (2014).
19. ATLAS User’s Manual, SILVACO Inc., Santa Clara, CA, USA, pp. 250–257 (2012).
20. H. Kato, S. Yamasaki, and H. Okushi, *Carrier compensation in (001) n-type diamond by phosphorus doping*, Diamond and Related Materials **16**(4–7), pp. 796–799 (2007).
21. P.-N. Volpe, J.-C. Arnault, N. Tranchant, G. Chicot, J. Pernot, F. Jomard, and P. Bergonzo, *Boron incorporation issues in diamond when TMB is used as precursor: Toward extreme doping levels*, Diamond and Related Materials **22**(2), 136–141 (2012).
22. O. A. Williams, M. Nesladek, M. Daenen, S. Michaelson, A. Hoffman, E. Osawa, K. Haenen, and R. B. Jackman, *Growth, electronic properties and applications of nanodiamond*, Diamond and Related Materials **17**(7–10), 1080–1088 (2008).
23. V.M. Placinta, L.N. Cojocariu, and C. Ravariu, *Test bench design for radiation tolerance of two ASICs*, Rom. J. Phys. **62**, 903 (2017).